Plant Science 338 (2024) 111897

Contents lists available at ScienceDirect

Plant Science

journal homepage: www.elsevier.com/locate/plantsci

# Maternal Embryo Effect Arrest 31 (MEE31) is a moonlighting protein involved in GDP-D-mannose biosynthesis and KAT1 potassium channel regulation

Adrián González-García [a], Maria Kanli [a], Natalia Wisowski [a], Eva Montoliu-Silvestre [a], Antonella Locascio [a], Alicia Sifres [a], Marcos Gómez [b], José Ramos [b], Rosa Porcel [a], Nuria Andrés-Colás [a], José Miguel Mulet [a], Lynne Yenush [a,*]

[a] Instituto de Biología Molecular y Celular de Plantas, Universitat Politècnica de València-Consejo Superior de Investigaciones Científicas, Valencia, Spain
[b] Departamento de Química Agrícola, Edafología y Microbiología, Edificio Severo Ochoa, Campus de Rabanales, Universidad de Córdoba, Córdoba, Spain

ARTICLE INFO

*Keywords:*
Potassium channel
Moonlighting protein
Stomatal regulation
Abiotic stress

ABSTRACT

Due to anthropogenic global warming, droughts are expected to increase and water availability to decrease in the coming decades. For this reason, research is increasingly focused on developing plant varieties and crop cultivars with reduced water consumption. Transpiration occurs through stomatal pores, resulting in water loss. Potassium plays a significant role in stomatal regulation. KAT1 is an inward-rectifying potassium channel that contributes to stomatal opening. Using a yeast high-throughput screening of an Arabidopsis cDNA library, MEE31 was found to physically interact with KAT1. MEE31 was initially identified in a screen for mutants with delayed embryonic development. The gene encodes a conserved phosphomannose isomerase (PMI). We report here that MEE31 interacts with and increases KAT1 activity in yeast and this interaction was also confirmed in plants. In addition, MEE31 complements the function of the yeast homologue, whereas the truncated version recovered in the screening does not, thus uncoupling the enzymatic activity from KAT1 regulation. We show that MEE31 overexpression leads to increased stomatal opening in Arabidopsis transgenic lines. Our data suggest that MEE31 is a moonlighting protein involved in both GDP-D-mannose biosynthesis and KAT1 regulation.

## 1. Introduction

Potassium is a major nutrient for plants, representing between 2% and 10% of plant dry weight (Leigh and Wyn Jones, 1984). At the cellular level, potassium accumulates in the plant cell cytosol at a concentration of about 100 mM and in variable amounts in the vacuole, but usually ranging from 10 to 200 mM, depending on the plant, tissue and the environmental conditions. Because potassium currents participate in stomatal movement, its homeostasis is essential for optimal water use efficiency. The opening of the stomatal pores involves increased proton efflux leading to potassium and anion uptake, while stomatal closing depends on potassium and anion efflux (Lawson and Blatt, 2014).

KAT1 and KAT2 are the main channels responsible for potassium uptake in guard cells, which form the stomata. These channels are composed of six transmembrane domains, one pore loop and four subunits. This family of potassium-selective channels are voltage-dependent and are responsible for the $K^+$ conductance of the plasma membrane in most cell types. Structural data obtained for related bacterial and mammalian channels and for KAT1 itself, indicate that this family adopts a homo- or heterotetrameric structure that forms the potassium pore (Jiang et al., 2003; Long et al., 2005; Li et al., 2020; Clark et al., 2020).

Studies of plant genome sequences reveal 3 families of genes encoding plasma membrane (PM) potassium transporters: the HKT family, the HAK/KUP/KT potassium transporter family and the channel family initially called Shaker, but renamed as Voltage-gated (VG) based on structural and phylogenetic studies (Corratgé-Faillie et al., 2010; Gierth and Mäser, 2007; Véry et al., 2003; Jegla et al., 2018). Among these, the two inward-rectifying channels (*KAT1* and *KAT2*) are mainly expressed in guard cells (*KAT2* is also expressed in leaf phloem) and are responsible for potassium uptake into these specialized cells and thus strongly influence stomatal movement. KAT1 can associate with KAT2

* Corresponding author.
*E-mail address:* lynne@ibmcp.upv.es (L. Yenush).

https://doi.org/10.1016/j.plantsci.2023.111897
Received 29 June 2023; Received in revised form 6 October 2023; Accepted 11 October 2023
Available online 17 October 2023

and also with other shaker channels, such as AKT1 and KC1 (Jeanguenin et al., 2011; Lebaudy et al., 2010). This difference in the composition of subunits is thought to confer different properties to the channel that may perform different physiological functions (Jeanguenin et al., 2011; Ivashikina et al., 2001; Xicluna et al., 2007). Several proteins have been identified that influence KAT1 activity. For example, KAT1 is phosphorylated by the $Ca^{2+}$-dependent protein kinase, CPK13 and the ABA-responsive Open Stomata 1 (OST1) kinase (Ronzier et al., 2014; Sato et al., 2009). The KAT1 channel has also been shown to bind to and be activated by 14–3–3 proteins (Sottocornola et al., 2006, 2008; Saponaro et al., 2017). Moreover, two types of SNARE (soluble N-ethylmaleimide-sensitive factor attachment protein receptor) proteins, the Qa SNARE SYP121 and the R-SNARE VAMP721, have been shown to physically interact with KAT1 and to modulate channel activity (Zhang et al., 2017; Honsbein et al., 2009; Hedrich et al., 2001; Sokolovski et al., 2008; Grefen et al., 2010). In the case of SYP121, it also participates in recycling of the channel to the PM after ABA-mediated internalization (Eisenach et al., 2012). These data clearly indicate that protein-protein interactions are a major regulatory mechanism for KAT1, and concomitantly for stomata regulation, water use efficiency and abiotic stress tolerance. Therefore, identifying additional proteins able to interact with KAT1 will likely reveal novel regulators of KAT1 function that represent novel participants in the molecular response mechanism to drought stress and serve as targets to develop novel biotechnological strategies to confer enhanced drought tolerance or resistance. Yeast is a good model system to identify protein-protein interactions with plant membrane proteins (Locascio et al., 2019a). Using the Split ubiquitin protein-protein interaction system, we have found novel regulatory proteins of KAT1, such as BAG4 (Locascio et al., 2019b). In this report, we describe a novel function for the Maternal Embryo Effect Arrest 31 protein, (hereafter MEE31) that we have identified as a KAT1 regulator using this strategy.

The *MEE31* gene, also known as *PMI1* (At3G02570) was identified in a genetic screening for mutants with delayed embryonic development (Pagnussat et al., 2005). *MEE31* presents a single splicing variant, which contains 5 exons and encodes for a 432 amino acid protein that encodes a conserved, zinc-dependent phosphomannose isomerase (PMI), which catalyzes the reversible isomerization between D-mannose-6-phosphate and D-fructose-6-phosphate (Maruta et al., 2008). The *MEE31* transcript and protein are detected in roots, stems, leaves and flowers throughout the entire plant and during both vegetative and reproductive growth (Maruta et al., 2008). These data agree with the data in the eFP Browser search engine (bar.utoronto.ca), which also indicates its expression in guard cells. Interestingly, *MEE31* gene expression and enzymatic activity show a diurnal pattern, as does KAT1 activity (Maruta et al., 2008; Lebaudy et al., 2008).

Regarding its function, as mentioned above, MEE31 is a phosphomannose isomerase. There are three classes of phosphomannose isomerases which are classified based on their sequence similarity (Proudfoot et al., 1994). The first of these classes (type 1), to which MEE31 belongs, includes all known PMIs in eukaryotes that share the YXDXNHKPE consensus sequence in their primary structure (Maruta et al., 2008; Coulin et al., 1993). Specifically, in *A. thaliana*, 2 genes belonging to this family have been identified, *MEE31* and *PMI2*, both of which are involved in the GDP-D-mannose biosynthesis pathway in plants (Kempinski et al., 2011). MEE31 appears to be the dominant isoform in most tissues and environmental conditions. GDP-mannose is involved in ascorbic acid biosynthesis, but this route requires only MEE31 (Maruta et al., 2008). Ascorbic acid plays an important role in plant development and the tolerance to abiotic stresses like temperature, water, salt and heavy metal stress (He et al., 2018; Tao et al., 2018). GDP-D-mannose is also required for other cellular functions, such as glycosylation, glycosylphosphatidylinositol (GPI)-anchoring, N-glycosylation of proteins and the synthesis of several structural cell wall polysaccharides (Abeijon and Hirschberg, 1992; Seifert, 2004). *MEE31* is an essential gene, as its inactivation leads to embryonic arrest (Pagnussat et al., 2005). Taken together, it is clear that *MEE31* affects a variety of pathways involved in development and stress responses.

Moonlighting proteins are defined as single polypeptide chains that are capable of carrying out two or more physiologically-relevant, but unrelated biological functions. In addition, to be classified as a moonlighting protein, these different functions must not be the result of gene fusion, alternate splicing or functions ascribed to different domains within the same protein (Jeffery, 1999). In some cases, they perform these different functions by using an active site pocket for catalysis and by interacting with other partners through a different part of their surface. Interestingly, many metabolic enzymes involved in glycolysis, glycerol metabolism and the TCA cycle exhibit moonlighting activities (Sriram et al., 2005). For example, Glyceraldehyde-3-phosphate dehydrogenase (GAPDH) has been reported to have several moonlighting activities, including the regulation of endocytosis and vesicular transport (Robbins et al., 1995; Tisdale, 2001). In plants, over 100 moonlighting proteins have been predicted to exist, mostly based on homology with proteins found in mammals or yeast (Su et al., 2019). Specific examples of experimentally-confirmed plant moonlighting proteins include the *HXK1* gene, encoding a hexokinase, which was shown to have roles in glucose sensing, independent of its catalytic activity in plants. More specifically, the kinase-dead mutant was shown to maintain signaling functions in physiological processes, such as leaf expansion and senescence, as well as root and inflorescence growth (Moore et al., 2003). Interestingly, hexokinase also acts as a glucose sensor in other organisms such as fungi, parasites and mammals, suggesting that moonlighting functions are evolutionarily conserved (Rodríguez-Saavedra et al., 2021). Other examples of plant moonlighting proteins include receptor like kinases and lipid kinases that also generate 3′,5′-cyclic guanosine monophosphate (cGMP) in plants (Turek and Irving, 2021).

Here, we present the identification and characterization of the MEE31 phosphomannose isomerase as a regulator of the KAT1 inward rectifying channel. Since this activity as a KAT1 regulator is independent of its phosphomannose isomerase enzymatic activity, our data indicate that the MEE31 is a novel plant moonlighting protein.

## 2. Materials and methods

### 2.1. Yeast strains, plasmids and functional complementation assays

For the Split-ubiquitin yeast two-hybrid assays, the THY.AP4 strain (MATa, *ura3, leu2, lexA::lacZ::trp1, lexA::HIS3, lexA::ADE2*; (Paumi et al., 2007) was transformed with the KAT1-pMetYCgate vector (ABRC CD3–815; (Obrdlik et al., 2004) or AKT1- and HAK5-Cub centromeric vectors constructed using the MoClo system (Lee et al., 2015) incorporating the promoter and Cub fusions present in pMetYCgate and the *LEU2* selection marker. *MEE31* full-length and N-terminal truncated (missing the first 69 amino acids) plasmids constructed using the MoClo system fusing a synthetic 3XHA-Nub sequence in the N-terminus in a YCp vector containing the *URA3* marker (Lee et al., 2015). To study the effect of the co-expression of *MEE31* on KAT1 activity, the *S. cerevisiae trk1 trk2* mutant strain (PLY240) was used (MATa *his3Δ200 leu2–3112 trp1Δ901 ura3–52 suc2Δ9 trk1Δ51 trk2Δ50::lox-KanMX-lox*; (Bertl et al., 2003)). This strain was transformed with the same plasmids used for the Split-ubiquitin assay. Growth was recorded after 72 h using a BioscreenC system (Oy Growth Curves Ab Ltd) in low potassium Translucent media (Navarrete et al., 2010) supplemented with 0.75 mg/mL methionine and/or KCl, as indicated. For the phosphomannose isomerase functional complementation, strain 1436–13 containing the *pmi40–101* mutant allele (Cullen et al., 2000) was transformed with plasmids constructed with the MoClo system (Lee et al., 2015) containing an N-terminal HIS6XFLAG3X tag in frame with the full-length or truncated versions of *MEE31* and incorporating a kanamycin resistance gene for selection of yeast transformants. Functional complementation assays were performed on solid YPD media with and without mannose supplementation.

### 2.2. Yeast protein extraction for immunodetection

For the protein extraction of *S. cerevisiae* samples for the Split-ubiquitin co-expression assays, 1 mL of culture with an $OD_{600}$ of 0.6 was collected and 90 μL of cold 100% (w/v) TCA was added and incubated for a minimum of 15 min on ice. The samples were centrifuged for 5 min at 13000 rpm at 4 °C. The residual medium was discarded and washed with 0.5 mL of cold acetone. The sample was centrifuged for 10 s and the acetone was removed. The pellets were dried using a speed-vac for 5 min at 37 °C to completely remove the acetone. Samples were stored at − 20 °C. Before use, the biomass was resuspended in urea buffer (25 mM Tris pH 6.8, 6 M Urea, 1% SDS w/v). The sample was shaken for 5 min on a bead beater in the presence of 0.1 mm glass beads. Laemmli buffer was added to the sample and it was mixed, and centrifuged for 3 min at 13000 rpm. The supernatant was transferred to a new tube and was used for the immunodetection assays.

### 2.3. $Rb^+$ uptake assay

To study the characteristics of $Rb^+$ uptake, the *S. cerevisiae trk1 trk2* mutant strain (PLY240) transformed with the same plasmids used for the Split-ubiquitin assay were used. Cells were potassium starved for three hours in low potassium Translucent media (Navarrete et al., 2010) supplemented with 0.75 mg/mL methionine. The cell samples were washed and suspended ($OD_{600\ nm}$ 0.3) in the uptake buffer [MES 10 mM supplemented with 2% glucose, $MgCl_2$ 0.1 mM and methionine 0.75 mg/mL at pH 5.8 adjusted with $Ca(OH)_2$]. 10 mM RbCl was added to the buffer at time zero and aliquots were withdrawn at the indicated times. The cells were then extracted with acid and the extracts analysed by atomic emission spectrophotometry (Ramos et al., 1990). Rubidium values are expressed as nanomoles per milligram dry weight of cells. These experiments were repeated twice with similar results and for two independent clones for each strain. Representative results corresponding to one of the experiments are shown.

### 2.4. Phosphomannose isomerase activity assay

The full-length and truncated versions of MEE31 containing an HIS6XFLAG3X tag were transformed into the BY4741 strain along with the empty vector control. Two independent clones of each strain were grown to $OD_{600}$ = 0.8 in 100 mLs of YPD + geneticin (200 μg/mL; Gibco). Proteins were extracted by vortexing in the presence of 0.1 mm glass beads (3 ×1 min) and were purified by affinity chromatography using Ni-NTA agarose (Macherey-Nagel) as indicated by the manufacturer (the elution buffer contained 250 mM imidazole). Phosphomannose isomerase activity was determined based on the previously published protocol with some modifications (Gracy and Noltmann, 1968). Briefly, 10 μL of purified protein was added to a coupled reaction containing 87 mM Tris pH 7.6, 5.5 mM D-mannose 6-phosphate, 0.45 mM nicotinamide adenine dinucleotide phosphate, 1.5 units phosphoglucose isomerase (all from Sigma-Aldrich), and 5 μg of glucose-6-phosphate dehydrogenase (Roche) in a total volume of 200 μL. Production of NADPH was monitored by measuring the absorbance at 25 °C in a flat-bottom 96 well plate at 340 nm in a TECAN spectrophotometer during 20 min. The assay was done in triplicate and the results for 2 biological replicates are shown. The amount of protein expressed was estimated after separation by SDS-PAGE by comparing the intensity of the direct blue staining to a BSA standard and the identity of the bands was confirmed by western blot using an anti-FLAG antibody (Sigma-Aldrich). Immune complexes were visualized using the corresponding anti-mouse HRP secondary antibody and ECL detection system (GE Healthcare).

*Plant Materials and Growth Conditions.* The following Arabidopsis (*Arabidopsis thaliana*) lines were employed: WT (Col-0), the *kat1* mutant (SALK 093506, carrying the T-DNA insertion in the first exon) obtained from the Salk Institute Genomic Analysis Laboratory. Arabidopsis plants were grown under an 8 h light/16 h dark photoperiod at 22 °C in 0.5x Murashige and Skoog (MS) media supplemented with 1% (w/v) Sucrose. *Nicotiana benthamiana* plants were grown for 4–5 weeks in soil under a 16 h light/8 h dark photoperiod at 24 °C. The floral dipping method was used to transform WT plants with the pDGB3 alpha1 GoldenBraid plasmids containing *KAT1-YFP* or *HA-MEE31t*, both under control of the cauliflower mosaic virus *CaMV 35 S* promoter and with the *Tnos* terminator using (Clough and Bent, 1998). Two independent T2 homozygous lines were used for the analyses.

### 2.5. Plant protein extraction

Protein extracts from leaves of 2 different homozygous *35 S::HA-MEE31t* lines and the WT control were collected from 4-week-old plants. 100 mg of biomass for each sample was collected and frozen in liquid nitrogen. The samples were crushed inside the tube with a pestle. Then 300 μL of protein extraction buffer (50 mM Tris pH 7.5, 5 mM EDTA, 150 mM NaCl, 20% glycerol (v/v), 1 mM PMSF, 1 complete™ Mini EDTA-free Protease Inhibitor Cocktail tablet, 0.15% NP-40 v/v) was added to the samples and incubated for 15 min at 4 °C. After the incubation the crude extract was separated from the biomass debris by filtering through a Whatman filter. 10 μL of the crude extract were mixed 1:1 with 5x LSB, separated on 10% SDS-PAGE gels, transferred to nitrocellulose and immunoblotted with the indicated antibodies (anti-HA, Roche; Anti-LexA, Abcam). For KAT1 detection, the crude extract was centrifuged for 1 h at 33000 rpm at 4 °C in a Beckman L-70 ultracentrifuge (Beckman Coulter, US, 80 Ti rotor). KAT1-YFP was detected using an anti-GFP antibody (PABG1, Chromotek) following the manufacture's recommendations. The anti-AHA3 antibody (kindly provided by Prof. Ramón Serrano (Campos et al., 1996)) was used as an internal control for equal protein loading and successful enrichment of the plasma membrane fraction. A 1:10,000 dilution of the antiserum was used. Immune complexes were visualized using the corresponding anti-mouse or anti-rabbit HRP secondary antibodies and ECL detection system (GE Healthcare).

### 2.6. Co-Immunoprecipitation

*Agrobacterium tumefaciens* (C58Ci) strains containing the pDGB3 alpha1_*35S::KAT1-YFP*, pDGB3 alpha1_*35S::MEE31t* or the pDGB3 omega1_*35S::KAT1-YFP_35S::MEE31t* plasmids were used for transient expression in *N. benthamiana*. An agrobacterium strain (C58Ci) transformed with the silencing suppressor P19 Tomato Bushy Stunt Virus was also used in the infiltration experiments (Sarrion-Perdigones et al., 2013). The KAT1-YFP protein was purified using the GFP-trap (ChromoTek GmbH) according to the manufacturer's indications. The beads were blocked for 30 min with *N. benthamiana* crude protein extract before starting the Co-IP, in order to avoid non-specific interactions with the resin. The Co-IP and crude extract samples were separated on 10% SDS-PAGE and analyzed by immunodetection of Western Blots using the anti-GFP antibody (PABG1, ChromoTek GmbH).

### 2.7. Fluorescence confocal microscopy

The abaxial part of the infiltrated leaves were analyzed 3 days post infiltration. For the visualization of the fluorescent proteins, an inverted laser scanning confocal microscope (Zeiss LSM780) was used, using the argon laser with a Plan-Apochromat 40x/1.20 WATER DIC M27 objective and the ZEN 2001 software (Zeiss). YFP fluorescence was visualized by exciting at $\lambda = 514$ and emission was analyzed at a range of $\lambda = 520–570$ nm. The autofluorescence of chloroplasts was detected at a range of $\lambda = 680–760$ nm. The emission peak of all fluorescent signals was confirmed. The images were processed with the Fiji software (Schindelin et al., 2012).

### 2.8. RT-qPCR

100 mg of the aerial part of 18-day-old plants grown in 0.5x MS media were collected and frozen in liquid $N_2$. Samples were ground by introducing 4–5 glass beads into each tube, and pulsing for 30 s at 30 Hz in a Retsch mixer mill, freezing the samples in liquid $N_2$ between pulses. The RNA extraction was performed using the NucleoSpin RNA Plant kit (Macherey-Nagel). cDNA was synthesized from 500 ng of RNA using the PrimeScript RT Reagent Kit (Takara Bio), using both oligo dT and random hexamer primers. The qPCR reactions were prepared with 5X PyroTaq EvaGreen qPCR Mix Plus (ROX; Cultek). The reactions were carried out in a QuantSudio 3 (ThermoFisher) using the following program: activation of the hot start DNApol and denaturation (15 min at 95 °C), 40 cycles of amplification (15 s at 95 °C, 30 s at 57 °C and 30 s at 72 °C) and melting curve (1 min at 60 °C, heating to 95 °C at 0.1 °C/s and 15 s at 95 °C). In the expression analysis, 3 technical replicates of each reaction were performed and the experiment was repeated two times. In each sample, the GAPDH gene was amplified as an endogenous control. The relative abundance of transcripts was calculated by using the $2-\Delta\Delta ct$ method (Livak and Schmittgen, 2001). The following primers were used: MEE31-FW TGGAGAAATGGGGTTGCGATC; MEE31-REV CCACAGAGAGCCTCGAATTGA; GAPDH-F CAATGAAGGACTGGAGAGGTG; GAPDH-R TCCCTTGAGTTTGCCTTCG; KAT1-YFP-F AATGCGGACAACGCTGAGAT; KAT1-YFP-R TGAACAGCTCCTCGCCCTT.

### 2.9. Stomatal opening assay

WT, *kat1,* 2 homozygous *35 S::KAT1-YFP* and 2 homozygous *35 S::HA-MEE31t* lines were grown for 3 days under short day conditions (8 h light and 16 h dark). Images of cotyledons were captured at the indicated times using a Leica DM5000 microscope equipped with a Leica DFC550 digital camera (magnification 20X). A minimum of 50 stomata from different plants of each genotype were measured at each time point using the Fiji software. One-way ANOVA analysis and Post-hoc Duncan's multiple range test were performed on all data sets. The significance level was established a $P < 0.05$ (Table S1) (Duncan, 1955). A Student's t test was also performed for the pairwise statistical analysis of the data.

## 3. Results

To identify regulators of the KAT1 inward-rectifying potassium channel of *A. thaliana*, we performed a high-throughput screening using the yeast Split-ubiquitin protein-protein interaction assay, as described (Locascio et al., 2019b). A truncated version of the *MEE31* gene lacking the coding sequence for the first 69 amino acids was recovered as a KAT1 interactor. To confirm this interaction, we re-transformed the plasmid recovered in the screening as well as the full-length version of MEE31 and the previously identified *BAG4* construct as a positive control. As shown in Fig. 1, we observed an interaction with KAT1 in all cases, except for the empty vector.

In order to begin to determine whether MEE31 co-expression has an effect on KAT1 activity, we co-transformed these same plasmids in a yeast strain lacking the endogenous potassium transporters Trk1 and Trk2. This strain grows poorly in media not supplemented with potassium and this growth defect can be recovered by expression of *KAT1* (Locascio et al., 2019b). To study the effect of *MEE31* co-expression, we took advantage of the regulatable promoter driving *KAT1* expression, which is repressed when methionine is added to the media. In this way, upon methionine supplementation, *KAT1* expression is low and this system provides a convenient readout for channel activation. As observed in Fig. 2A, both the truncated and full-length versions of MEE31 improve growth in liquid media with limiting potassium and methionine supplementation (low KAT1 expression). Given that the controls show the expected results and the protein expression of each transformed strain is similar (Fig. 2B), these data suggest that both isoforms of MEE31 can activate KAT1 channel activity in yeast. We confirmed this observation by measuring $Rb^+$ uptake in these same strains. As observed in Fig. 2C, the co-expression of either the full-length or the truncated version of MEE31 markedly improved $Rb^+$ uptake in these strains. These data prove that MEE31 co-expression improves KAT1 activity.

We next tested the ability of the full-length and truncated versions of MEE31 to functionally complement the slow growth phenotype of strain lacking its yeast homologue (*PMI40*). This strain displays slow growth in the absence of mannose supplementation to the media (Cullen et al., 2000). As observed in Fig. 3A, only the full-length version of MEE31 was able to improve the growth of the *pmi40–101* strain in media without mannose supplementation, while expression of the truncated version (MEE31t) had no effect. We confirmed the correct expression of the MEE31 isoforms by immunodetection (Fig. 3B). We corroborated this result in vitro by performing a coupled reaction using the full-length and truncated versions of MEE31 purified by affinity chromatography from yeast, as described in Materials and Methods. As shown in Fig. 3C, the production of NADPH was only observed for full-length MEE31. The enzymatic activity for the two biological replicates for the purified full-length versions was estimated to be 870 and 1150 μmoles/min/mg purified protein, whereas the activity of the truncated versions and the empty vector were essentially identical. This specific activity is in good agreement with previous results (Gracy and Noltmann, 1968). Our results clearly demonstrate that the full-length MEE31 has enzymatic activity in yeast and in vitro, whereas the activity of the truncated version is undetectable. This is very interesting because it allows for the separation of the enzymatic function and the ability to interact with and activate the KAT1 channel. Full-length MEE31 maintains both functions,

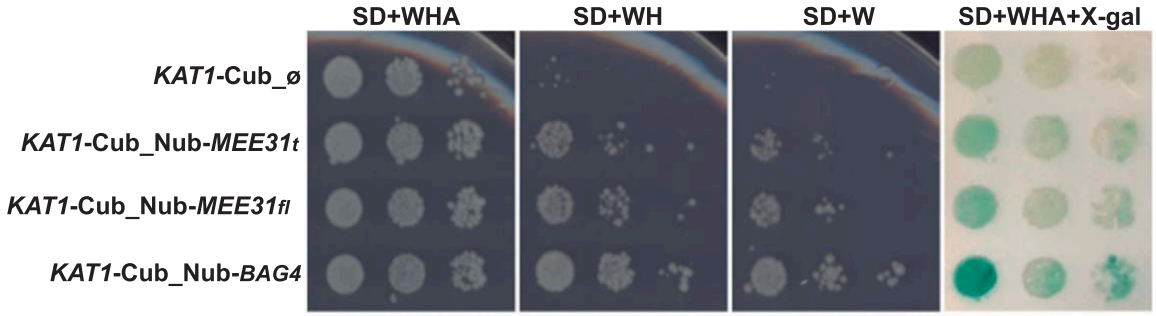


**Fig. 1.** Split-ubiquitin protein-protein interaction assay. The THY.AP4 yeast strain was co-transformed with the KAT1-Cub vector and the plasmids indicated on the left. Saturated cultures were spotted onto the indicated media and growth was recorded after 72 h. Similar results were observed in 4 independent colonies for each combination. W, tryptophan; H, histidine; A, adenine refer to the components added to the SD (Synthetic Dextrose) media used for the analysis. Strains growing on plates lacking H and/or A or showing a blue color in plates containing X-gal represent combinations where protein-protein interactions are observed. MEE31t refers to the truncated version of the gene recovered in the screening. It lacks the first 69 amino acids. Fl, full-length. Ø, empty vector. Nub-BAG4 was used as a positive control (Locascio et al., 2019b).

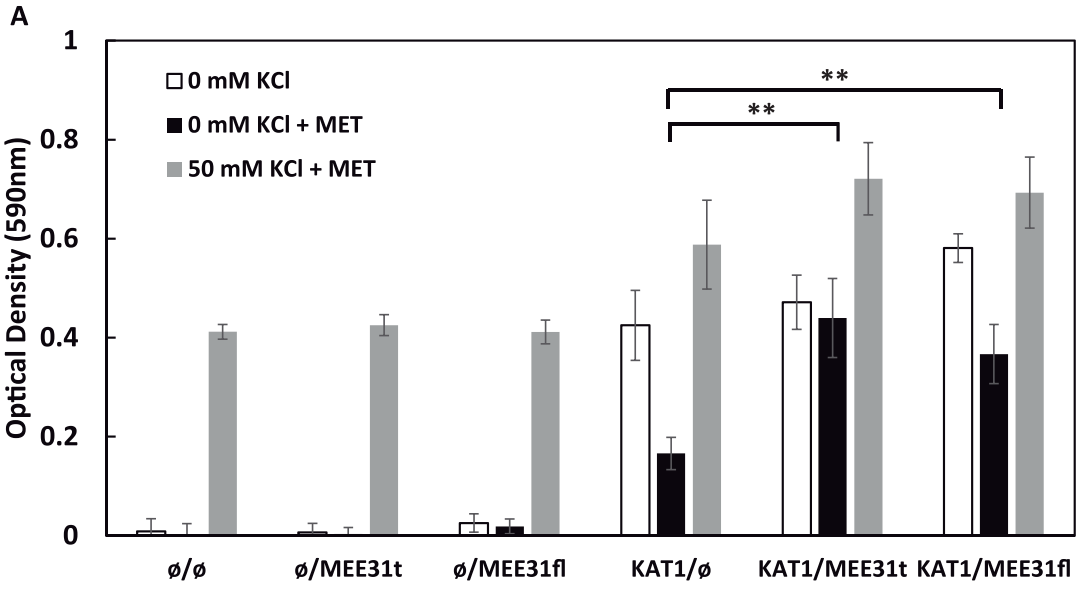


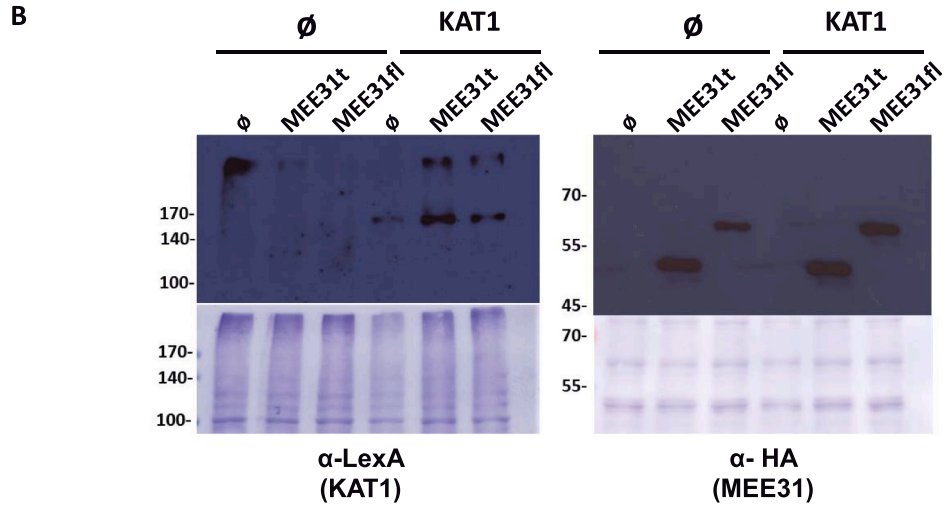


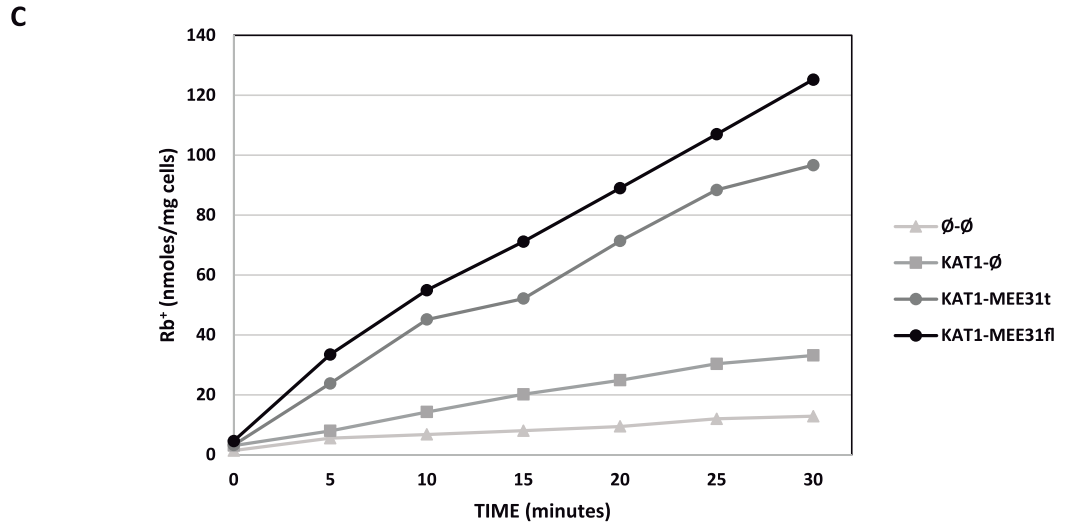


*(caption on next page)*

**Fig. 2.** Effect of MEE31 isoform co-expression on KAT1 activity in yeast. A. The indicated plasmids were co-transformed in the *trk1 trk2* mutant strain (PLY240). Growth assays were performed as described in Materials and Methods using Translucent media (12 μM KCl) with or without methionine supplementation to control the expression of KAT1 (*MET25* promoter). The graph shows the average value of the optical density at 72 h for triplicate determinations and the experiment was done with at least 3 independent transformants for each plasmid combination. (0 mM KCl: Translucent media with no KCl supplementation (limiting $K^+$ and high KAT1 expression); 0 mM KCl + MET: Translucent media without KCl, containing 0.75 mg/mL methionine (limiting $K^+$, low KAT1 expression); 50 mM KCl: Translucent media with 50 mM KCl, containing 0.75 mg/mL methionine (non-limiting $K^+$, low KAT1 expression)). Data presented are the mean ± SD. Asterisks (**) indicate statistical significance (Student's t test) with $P \leq 0.01$. B. The correct expression of each of the fusion proteins was confirmed by immunoblot analysis of protein extracts from the indicated strains. The KAT1 is detected with the anti-LexA antibody and the prey proteins with the anti-HA antibody. Results for a representative clone are shown. The Direct Blue staining is shown as a loading control. MEE31fl, full-length. MEE31t, truncated version. Ø, empty vector. C. The indicated plasmids were co-transformed in the *trk1 trk2* mutant strain (PLY240) and $Rb^+$ uptake was determined as described in Materials and Methods.

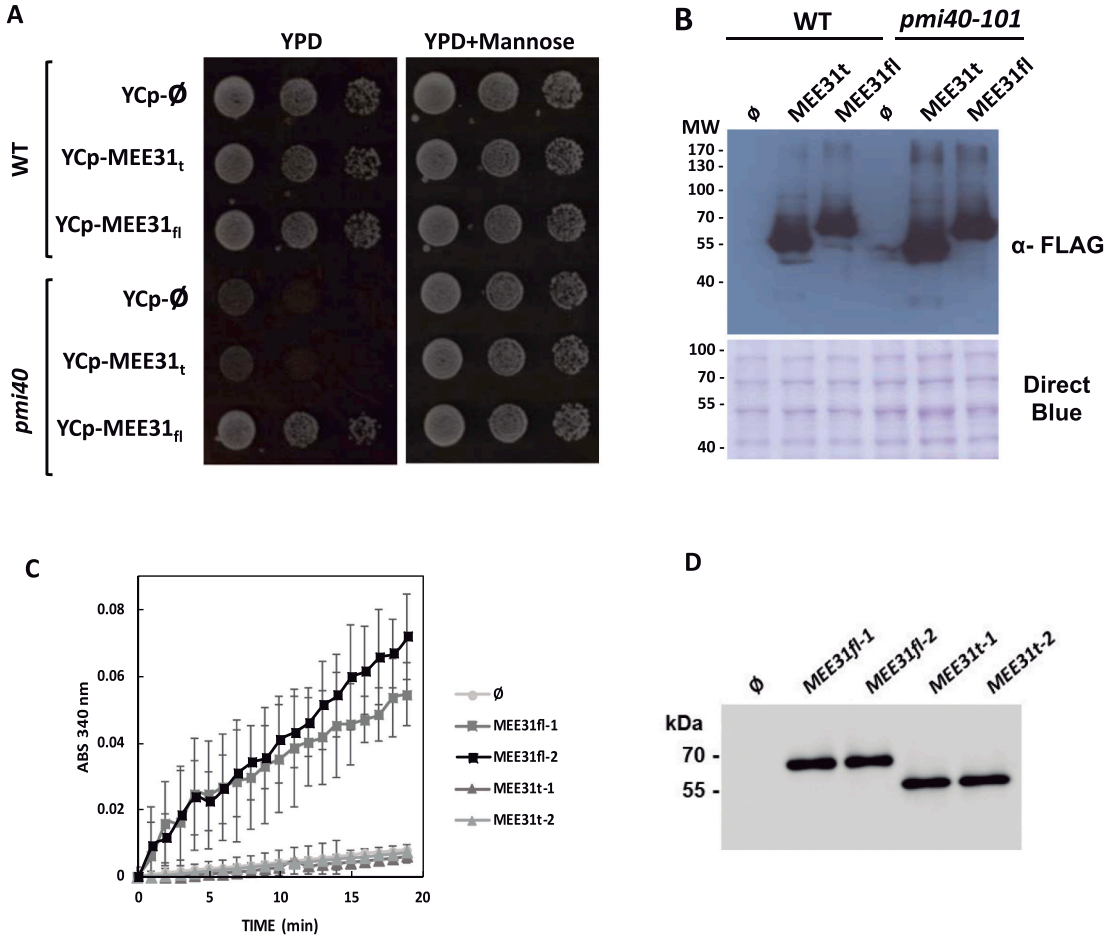


**Fig. 3.** Analysis of the functional complementation in yeast and in vitro activity of MEE31. A. The *pmi40–101* yeast mutant strain lacking the *MEE31* homologue was transformed with the indicated plasmids. Saturated cultures were spotted onto the indicated media and growth was recorded after 72 h. Similar results were observed in 4 independent colonies for each transformation. B. Immunoblot analysis of protein extracts from the indicated strains showing the correct expression of the MEE31 isoforms (anti-FLAG). Results for a representative clone are shown. The Direct Blue staining is shown as a loading control. C. MEE31 versions harboring a HIS6XFLAG3X tag were purified from yeast using affinity chromatography and the enzymatic activity of the MEE31 versions was determined by monitoring NADPH production of a three-way coupled reaction, as described in Materials and Methods. The graph depicts the time course of the mean of the absorbance ± SD of triplicate determinations of 2 biological replicates for each version of MEE31 (MEE31fl and MEE31t) and the empty vector control. D. Immunoblot analysis of proteins purified from the indicated strains showing the correct expression of the MEE31 isoforms (anti-FLAG). MEE31t refers to the truncated version of the gene recovered in the screening. fl, full-length. Ø, empty vector.

whereas the truncated version acts only as a KAT1 regulator.

According to the Uniprot database, amino acids 124, 126, 151, and 288 are predicted to directly coordinate the zinc ion and arginine 307 is predicted to be the catalytic residue (Swan et al., 2004; Bateman et al., 2021). All of these residues are maintained in the truncated version of MEE31 recovered in the screening, but, as our data shows, the truncated version of MEE31 cannot functionally complement the yeast mutant lacking the homologous gene. We performed a comparison of the structures of both isoforms generated using AlphaFold2 (Mirdita et al., 2022). The truncated version is predicted to have a structure identical to the full-length protein. Moreover, the first 30 amino acids of the full-length protein are unstructured and so unlikely to perform a defined function. We used the Chimera package from the Computer Graphics Laboratory, UCSF (Pettersen et al., 2004) to compare the two predicted structures (Fig. 4). According to the structural analysis provided in Conserved Domain Database (Lu et al., 2020), the first three (W32, E61 and W63) of the 17 amino acids predicted to be involved in the formation of the full active site are missing in the truncated version, while the rest of the amino acids and the configuration of the active site remain intact. Based on similarity to the *C. albicans* structure, these two tryptophan residues are predicted to be close to the entrance of the zinc binding site and to be important for zinc binding (Cleasby et al., 1996).

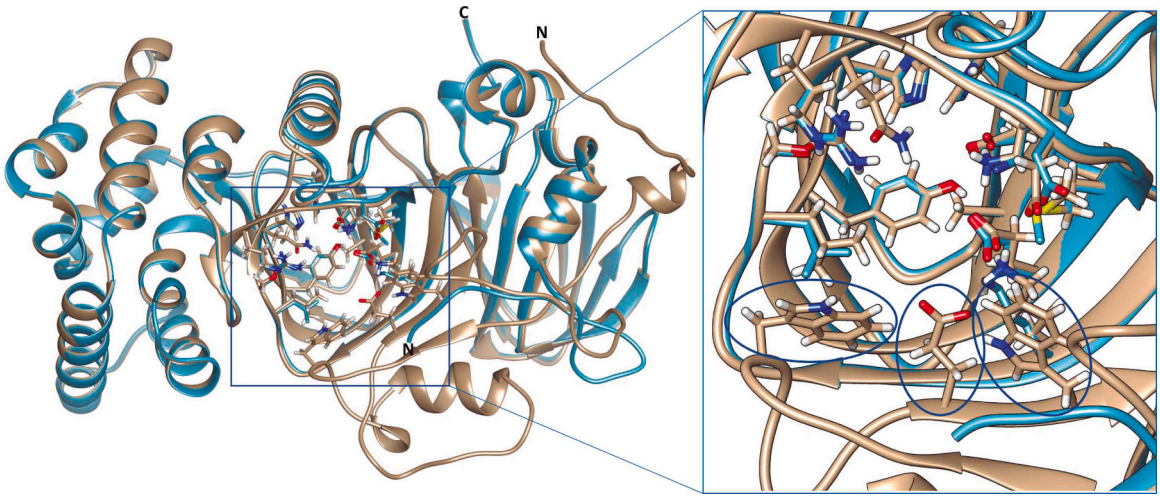


**Fig. 4.** Prediction of the 3D structures of the MEE31 isoforms using AlphaFold2. Prediction of the 3D structures of the MEE31 isoforms using AlphaFold2.ipynb. An overlay of the full-length MEE31 (beige) and the truncated version (blue) recovered in the screening (missing aa's 1–69) is shown (left). The residues implicated in the formation of the catalytic site are shown in ball and stick mode, while the rest is shown as a ribbon diagram. The first 30 amino acids are predicted to be unstructured and the rest of the missing region seems to form a discreet region (bottom), including 3 residues (circled) important for the catalytic function (W32, E61 and W63; right). The core structure and the rest of the catalytic residues are conserved in the truncated version. The figure was made using the Chimera package from the Computer Graphics Laboratory, UCSF. N and C denote the N- and C-termini of the proteins.

Therefore, if these residues are missing, zinc binding and thus catalytic activity are likely to be affected. This is in good agreement with the functional complementation and in vitro data presented here showing that the activity of the truncated version is undetectable. Importantly, our protein-protein interaction and KAT1 activity assays show that this truncated version binds to and activates the channel in yeast. In this way, we are able to separate the enzymatic activity from KAT1 regulation.

Based on these results, we chose to continue our analyses with the truncated version of MEE31 to mitigate possible artefacts caused by the overexpression of a metabolic enzyme. We first wanted to confirm the interaction between KAT1 and MEE31 in plants. To this end, we transiently expressed *KAT1-YFP* and an HA-tagged version of *MEE31t* in *N. benthamiana*. Co-immunoprecipitation analysis showed a robust interaction between MEE31t and KAT1, thus confirming a physical interaction in plants (Fig. 5A). We employed Bimolecular Fluorescence Complementation (BiFC) as a complementary approach. As observed in Fig. 5B, we observed a clear signal in the cell periphery upon co-expression of *KAT1* and *MEE31t*, similar to that observed for the samples detecting the KAT1-KAT1 interaction in the homo or heterotetramer that we used as a positive control (Fig. 5C). No signal was observed for the negative control expressing MEE31t or KAT1 co-expressed with the corresponding fusions with unrelated proteins (Fig. 5D-E).

Having confirmed the interaction between KAT1 and MEE31t in plants, we generated transgenic *A. thaliana* lines overexpressing HA-*MEE31t* in order to analyze phenotypes related to KAT1 activity that would allow us to determine if MEE31t may regulate the channel in a plant model system. Two homozygous transgenic lines expressing MEE31t were analyzed for gene and protein expression. As shown in Fig. S1A, lines with varying amounts of *MEE31t* expression were identified (between 2 and 7-fold overexpression). There was a clear correlation with the amount of accumulation of the MEE31t protein (Fig. S1C). A similar approach was carried out to generate transgenic lines overexpressing KAT1 (Figs. S1B and D).

To begin to ascertain the effect of MEE31t overexpression on KAT1 activity in *planta*, we studied the stomatal opening of the stable homozygous *35 S::HA-MEE31t* lines, alongside WT, *kat1* and homozygous *35 S::KAT1-YFP* lines in response to light. We have previously observed a delay in stomatal opening in response to light in plants lacking the *KAT1* gene (Locascio et al., 2019b). In Fig. 6, the results of the analysis of the *35 S::MEE31t* lines are shown together with control lines lacking or overexpressing *KAT1*. Interestingly, we observed that the *MEE31t* overexpressing lines showed increase stomatal aperture under dark conditions (time 0) and the stomatal closure was delayed, very similar to what we observed for the KAT1 overexpressing lines (Rovira et al.,), Fig. 6 and Table S1). This data shows that the overexpression of *MEE31t* leads to increased stomatal opening, which is consistent with increased inward-rectifying potassium channel activity, although we cannot discard additional mechanisms at this stage.

## 4. Discussion

In a high-throughput screening for KAT1 interactors, we isolated a protein encoded by a truncated version of the *MEE31* gene. The clone recovered is missing the sequence encoding the first 69 amino acids of MEE31. Our studies of structural models reveal that although the conserved residues of the YXDXNHKPE motif and other catalytically-relevant residues characteristic of type I phosphomannose isomerases remain intact in this MEE31 isoform, elements of the catalytic pocket are missing. More specifically, the truncated version lacks two conserved tryptophan residues that are predicted to be close to the entrance of the zinc binding site and so are likely to affect the affinity of zinc binding and consequently the catalytic activity. This hypothesis is supported by our observations that this truncated version has undetectable activity in vitro and is unable to complement the yeast mutant, whereas the full-length version shows in vitro activity and robust complementation. Thus, these data demonstrate that the binding and regulation of KAT1 activity can be separated from the catalytic activity of MEE31.

In humans, the Carbohydrate-Deficient Glycoprotein (CDG) Syndrome type 1b has been shown to be caused by mutations in the human *MPI* gene encoding phosphomannose isomerase. This syndrome is a gastrointestinal disorder characterized by protein-losing enteropathy (Niehues et al., 1998; Jaeken et al., 1998). These patients can also present thrombosis as well as life-threatening bleeding and are treated with oral administration of mannose. In the case of the mouse homologue, it was shown that ablation of the gene encoding this enzyme led to mannose 6-phosphate accumulation, which results in inhibition of glucose metabolism and depletion of intracellular ATP and leads to embryonic lethality (DeRossi et al., 2006). *MEE31* is also an essential gene in Arabidopsis (Pagnussat et al., 2005). As mentioned, *MEE31* was

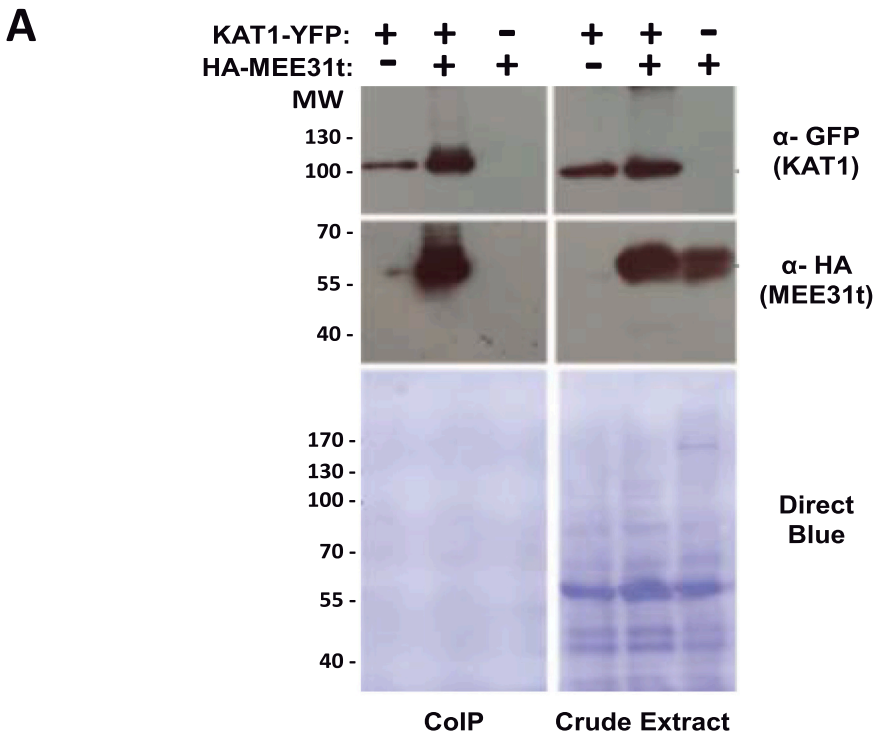


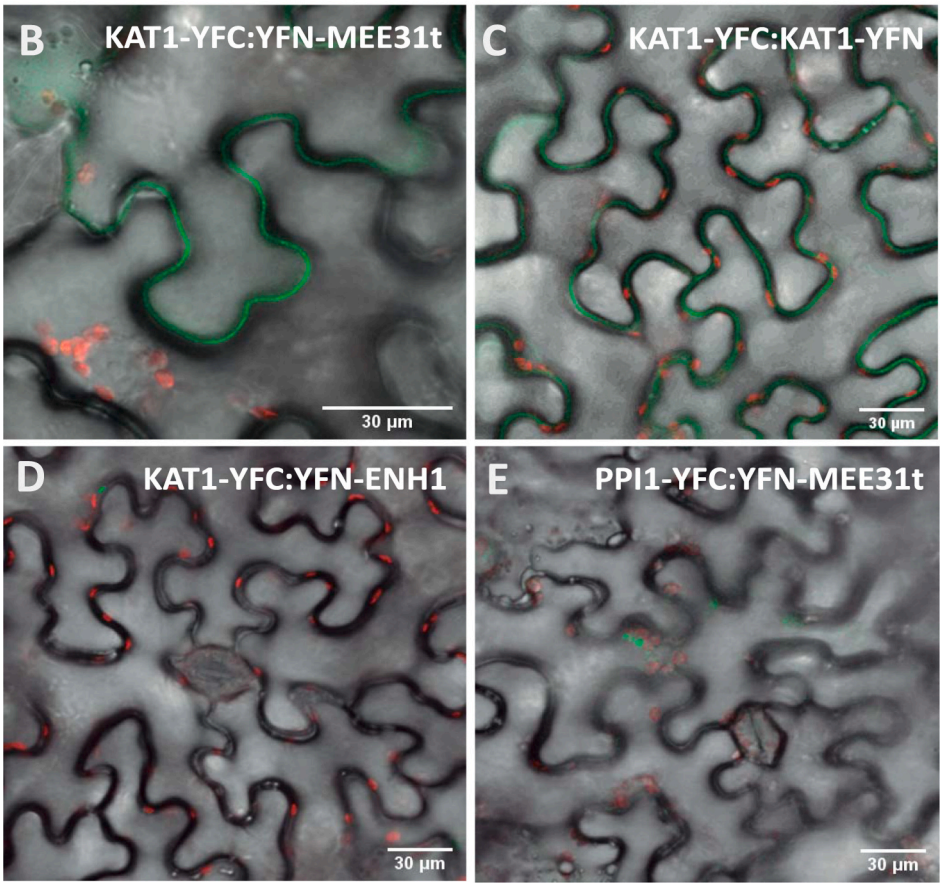


(caption on next page)

**Fig. 5.** Confirmation of the KAT1-MEE31 interaction in plants. A. Co-immunoprecipitation assay between KAT1-YFP and HA-MEE31t. *N. benthamiana* leaves were infiltrated with the Agrobacterium strains harboring the indicated plasmids and samples for protein extraction were harvested after 72 h. The α-HA immunoblot detects MEE31t and the α-GFP immunoblot detects KAT1. The interaction is shown in lane 2. The molecular weight markers are shown on the left and the Direct Blue staining is shown as a loading control. B-E. Agrobacterium strains harboring the indicated plasmids were used to infiltrate *N. benthamiana* leaves, and images were obtained using fluorescence confocal microscopy 72 h post-infiltration. B. Representative BiFC images for the KAT1-MEE31t interaction. Representative BiFC images for the KAT1-KAT1 interaction are shown in part C. D and E. Representative images of the corresponding negative controls. For B-E, similar results were observed in at least two independent experiments performed on different days. Scale bars = 30 μm. IP, immunoprecipitation; PPI1, Proton Pump Interacting-1; ENH1, Enhancer of SOS3–1; YFC, C-terminal part of YFP; YFN, N-terminal part of YFP.

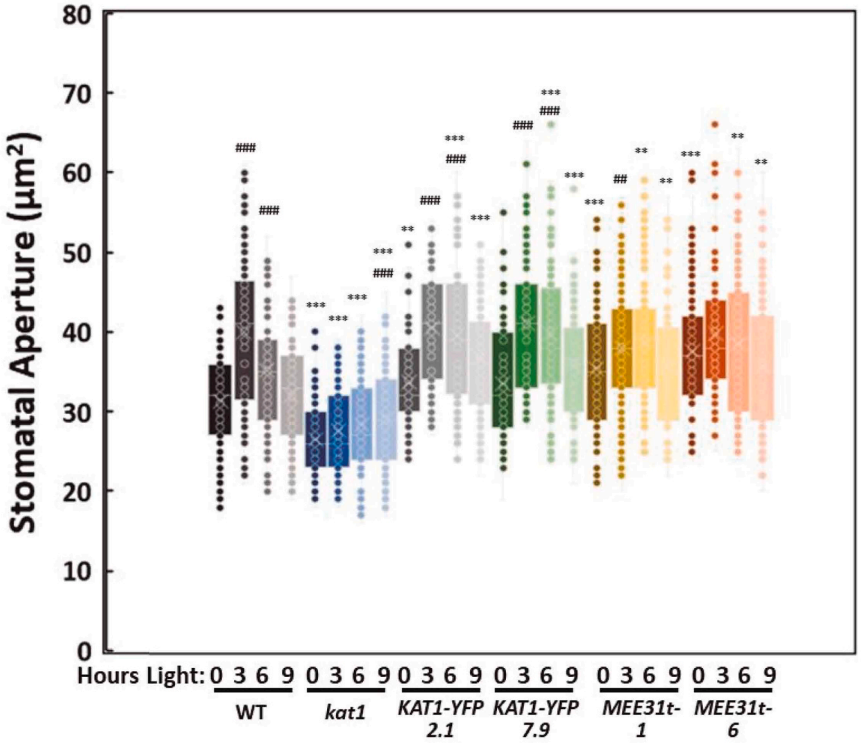


**Fig. 6.** Stomatal opening assay of *A. thaliana* lines overexpressing MEE31t. Time course analysis of stomatal opening for the indicated lines was analyzed in 3-day-old cotyledons grown under short day conditions and imaged before (time 0) and at the indicated times after the lights turned on. The area of 50–100 stomata from different plants of each genotype was measured using the Fiji software. The box-whisker plots contain all data points and the boxes extend from the first quartile to the third quartile. The whiskers indicate the minimum and maximum values. The central lines show the average and x represents the median values. Data points outside the boxes are outliers. Statistical pairwise analyses were performed using the Student's t test. ## indicates $P \leq 0.01$ and ### indicates $P \leq 0.001$ for differences as compared to the dark control for each genotype and * * indicates $P \leq 0.01$ * ** and indicates $P \leq 0.001$ when comparing with the WT control for the same time point. Additional statistical analyses of these data are described in Materials and Methods and presented in Table S1.

initially identified in a genetic screen for mutants with delayed embryonic development. The cause of this phenotype has yet to be identified in plants, but is may due to the toxic effects of mannose 6-phosphate accumulation as well, as it has been shown to inhibit key enzymes, such as hexokinase, phosphoglucose isomerase, and glucose-6-phosphate dehydrogenase, all highly conserved and essential for glucose metabolism. Another possibility is the defect in protein glycosylation, since it has been shown that a temperature-sensitive mutation in the phosphomannomutase (PMM) gene, which is downstream of MEE31, disrupts protein glycosylation and leads to cell death (Hoeberichts et al., 2008).

It is interesting to note that reduction of MEE31 function using RNA interference has also been shown to reduce ascorbic acid accumulation, since this metabolite is formed from GDP-mannose through the D-mannose/L-galactose (D-Man/L-Gal) pathway (Maruta et al., 2008; Conklin et al., 1999; Wheeler et al., 1998). Levels of this antioxidant molecule increase in response to environmental stresses, including light, temperature, salt and drought stress, the presence of atmospheric pollutants, metals and herbicides (Davey et al., 2000). As discussed, GDP-mannose is also a key metabolite involved in protein glycosylation, since mannose, derived from GDP-Man, is a crucial building block of the core glycan chain attached to the modified proteins (Hoeberichts et al., 2008; Lerouge et al., 1998; Spiro, 2002). Although we observed that the inactive form of MEE31 was still able to bind to and regulate KAT1, we wanted to discard a role for protein glycosylation. Therefore, we analyzed the KAT1 primary sequence and the structural model (Li et al., 2020) to identify possible extracellular N-linked glycosylation sites. Asparagine 158 is the only one located in an N-X-S/T consensus site in the extracellular part of the channel. We mutated this asparagine to glutamine and examined the banding pattern in Western blots of KAT1-YFP transiently expressed in *N. benthamiana*. We did not observe any changes in the pattern of high molecular weight bands as compared to the wild type control (data not shown). Therefore, we propose that MEE31-mediated KAT1 regulation does not involve this type of post-translation modification.

Here, we show a robust physical interaction between MEE31 and KAT1 in plants and that the overexpression of the full-length and the catalytically-defective truncated version leads to increased KAT1 activity and increased and prolonged stomatal aperture, similar to lines overexpressing *KAT1*. This phenotype, taken together with the rest of our results, strongly suggests that MEE31t is acting as a KAT1 regulator in vivo. Since this truncated version of MEE31 has reduced enzymatic

activity, our data suggest that MEE31 is a moonlighting protein involved in GDP-mannose biosynthesis and KAT1 channel regulation. MEE31 is predicted to be a cytosolic protein (https://suba.live/suba-app/factsheet.html?id=AT3G02570) and we confirmed this data in transient expression assays in *N. benthamiana* using YFP-fused versions. Therefore, MEE31 would be available to bind to the cytosolic loops and domains of KAT1.

Other examples of KAT1 regulators with additional cellular functions have been reported. More specifically, Qa SNARE SYP121 and the R-SNARE VAMP721, two types of SNARE (soluble N-ethylmaleimide-sensitive factor protein attachment protein receptor) proteins, have been shown to modulate KAT1 channel activity through a direct physical interaction (Honsbein et al., 2009; Sokolovski et al., 2008; Grefen et al., 2010; Honsbein et al., 2011; Zhang et al., 2015; Lefoulon et al., 2018). Both of these proteins have been postulated to directly regulate KAT1 gating, but in opposing manners (SYP121 activates/VAMP721 inhibits). Interestingly, trafficking and gating functions of SYP121 have been shown to be physically separable using mutational studies (Zhang et al., 2017, 2015). Therefore, these KAT1 regulators may also be considered to be moonlighting proteins.

One outstanding question is the molecular mechanism by which MEE31 is able to regulate KAT1 activity. More experiments will be required to determine the mechanism involved in MEE31-mediated KAT1 regulation in plants. This phenotype would be difficult to assess using transient overexpression assays in plants and will require alternate approaches that guarantee physiological expression levels of both proteins. Since *MEE31* is an essential gene, using loss-of-function mutant lines is not an option.

On the other hand, it has been reported that the MEE31 protein interacts physically with CHC2, the heavy chain of clathrin (At3g08530) (Arabidopsis Interactome Mapping Consortium, 2011). CHC2 has been implicated in endocytosis (Chen et al., 2011), intracellular traffic and also stomatal movements (Larson et al., 2017). In this context, it is interesting to point out that the hormone abscisic acid (ABA) controls the selective endocytosis of the KAT1 potassium channel, through an undefined molecular mechanism (Sutter et al., 2007). Once internalized in vesicles upon ABA treatment, it has been observed that instead of being degraded in the vacuole, KAT1 remains in vesicles and is recycled to the plasma membrane when ABA levels decrease. Given its interaction with both CHC2 and KAT1, MEE31 could be a key element in the mechanism of ABA-mediated endocytosis of KAT1. Future studies will address this interesting possibility and other possible regulatory mechanisms.

Here, we have identified MEE31 as a moonlighting protein involved in both GDP-mannose biosynthesis and KAT1 channel regulation. This work adds yet another metabolic enzyme to the list of proteins involved in carbohydrate metabolism with additional functions. Further work is required to define the molecular mechanism of this regulation, but our results add another player in the regulation of an inward-rectifying potassium channel expressed on the plasma membrane of guard cells. Thus, elucidation of this regulatory mechanism could provide insights important for further understanding stomatal movement.

## Funding

This work was supported by grant PID2019-104054GB-I00 financed by the Ministerio de Ciencia e Innovación, Spain (MCIN/AEI/10.13039/501100011033).

## CRediT authorship contribution statement

**LY:** Conceptualization, Funding acquisition, Methodology, Project administration, Resources, Supervision, Writing – original draft**,** Investigation, Methodology, Writing – review & editing, Data curation, Formal analysis**. JMM:** Conceptualization, Funding acquisition, Methodology, Project administration, Resources, Supervision, Writing – original draft. **AG-G, NW, MK, AS, MG, JR, NA-C, AL:** Investigation, Methodology, Writing – review & editing. **RP:** Data curation, Formal analysis, Investigation, Methodology, Writing – review & editing.

## Declaration of Competing Interest

The authors declare that they have no known competing financial interests or personal relationships that could have appeared to influence the work reported in this paper.

## Data Availability

Data will be made available on request.

## Acknowledgments

Maria Pilar López and Marisol Gascón are acknowledged for excellent technical assistance. Dr. Dolores Bernal, Dr. Amparo Pascual-Ahuir and Dr. Maria Adelaida García are acknowledged for providing reagents and for helpful discussions.

## Appendix A. Supporting information

Supplementary data associated with this article can be found in the online version at doi:10.1016/j.plantsci.2023.111897.

## References

R.A. Leigh, R.G. Wyn Jones, A hypothesis relating critical potassium concentrations for growth to the distribution and functions of this ion in the plant cell, N. Phytol. 97 (1984) 1–13, https://doi.org/10.1111/J.1469-8137.1984.TB04103.X.

T. Lawson, M.R. Blatt, Stomatal size, speed, and responsiveness impact on photosynthesis and water use efficiency, Plant Physiol. 164 (2014) 1556–1570, https://doi.org/10.1104/pp.114.237107.

Y. Jiang, A. Lee, J. Chen, V. Ruta, M. Cadene, B.T. Chait, R. MacKinnon, X-ray structure of a voltage-dependent K+ channel, Nature 423 (2003) 33–41, https://doi.org/10.1038/nature01580.

S.B. Long, E.B. Campbell, R. Mackinnon, Crystal structure of a mammalian voltage-dependent Shaker family K+ channel, Science 309 (1979) (2005) 897–903, https://doi.org/10.1126/science.1116269.

S. Li, F. Yang, D. Sun, Y. Zhang, M. Zhang, S. Liu, P. Zhou, C. Shi, L. Zhang, C. Tian, Cryo-EM structure of the hyperpolarization-activated inwardly rectifying potassium channel KAT1 from Arabidopsis, Cell Res. 2020 30:11 30 (2020) 1049–1052, https://doi.org/10.1038/s41422-020-00407-3.

M.D. Clark, G.F. Contreras, R. Shen, E. Perozo, Electromechanical coupling in the hyperpolarization-activated K + channel KAT1, Nature 583 (2020) 145, https://doi.org/10.1038/s41586-020-2335-4.

C. Corratgé-Faillie, M. Jabnoune, S. Zimmermann, A.A. Véry, C. Fizames, H. Sentenac, Potassium and sodium transport in non-animal cells: the Trk/Ktr/HKT transporter family, Cell Mol. Life Sci. 67 (2010) 2511–2532, https://doi.org/10.1007/s00018-010-0317-7.

M. Gierth, P. Mäser, Potassium transporters in plants–involvement in K+ acquisition, redistribution and homeostasis, FEBS Lett. 581 (2007) 2348–2356, https://doi.org/10.1016/j.febslet.2007.03.035.

A.A. Véry, H. Sentenac, A.A. Very, H. Sentenac, Molecular mechanisms and regulation of K+ transport in higher plants, Annu Rev. Plant Biol. 54 (2003) 575–603, https://doi.org/10.1146/annurev.arplant.54.031902.134831.

T. Jegla, G. Busey, S.M. Assmann, Evolution and structural characteristics of plant voltage-gated K+ channels, Plant Cell 30 (2018) 2898, https://doi.org/10.1105/TPC.18.00523.

L. Jeanguenin, C. Alcon, G. Duby, M. Boeglin, I. Chérel, I. Gaillard, S. Zimmermann, H. Sentenac, A.A. Véry, AtKC1 is a general modulator of Arabidopsis inward Shaker channel activity, Plant J. 67 (2011) 570–582, https://doi.org/10.1111/j.1365-313X.2011.04617.x.

A. Lebaudy, F. Pascaud, A.A. Véry, C. Alcon, I. Dreyer, J.B. Thibaud, B. Lacombe, Preferential KAT1-KAT2 heteromerization determines inward K+ current properties in Arabidopsis guard cells, J. Biol. Chem. 285 (2010) 6265–6274, https://doi.org/10.1074/jbc.M109.068445.

N. Ivashikina, D. Becker, P. Ache, O. Meyerhoff, H.H. Felle, R. Hedrich, K(+) channel profile and electrical properties of Arabidopsis root hairs, FEBS Lett. 508 (2001) 463–469.

J. Xicluna, B. Lacombe, I. Dreyer, C. Alcon, L. Jeanguenin, H. Sentenac, J.B. Thibaud, I. Chérel, Increased functional diversity of plant K+ channels by preferential heteromerization of the shaker-like subunits AKT2 and KAT2, J. Biol. Chem. 282 (2007) 486–494, https://doi.org/10.1074/jbc.M607607200.

E. Ronzier, C. Corratgé-Faillie, F. Sanchez, K. Prado, C. Brière, N. Leonhardt, J. B. Thibaud, T.C. Xiong, CPK13, a noncanonical Ca2+-dependent protein kinase,

specifically inhibits KAT2 and KAT1 shaker K+ channels and reduces stomatal opening, Plant Physiol. 166 (2014) 314–326, https://doi.org/10.1104/pp.114.240226.
A. Sato, Y. Sato, Y. Fukao, M. Fujiwara, T. Umezawa, K. Shinozaki, T. Hibi, M. Taniguchi, H. Miyake, D.B. Goto, N. Uozumi, Threonine at position 306 of the KAT1 potassium channel is essential for channel activity and is a target site for ABA-activated SnRK2/OST1/SnRK2.6 protein kinase, Biochem. J. 424 (2009) 439–448, https://doi.org/10.1042/BJ20091221.
B. Sottocornola, S. Visconti, S. Orsi, S. Gazzarrini, S. Giacometti, C. Olivari, L. Camoni, P. Aducci, M. Marra, A. Abenavoli, G. Thiel, A. Moroni, The potassium channel KAT1 is activated by plant and animal 14-3-3 proteins, J. Biol. Chem. 281 (2006) 35735–35741, https://doi.org/10.1074/jbc.M603361200.
B. Sottocornola, S. Gazzarrini, C. Olivari, G. Romani, P. Valbuzzi, G. Thiel, A. Moroni, 14-3-3 proteins regulate the potassium channel KAT1 by dual modes, Plant Biol. 10 (2008) 231–236, https://doi.org/10.1111/j.1438-8677.2007.00028.x.
A. Saponaro, A. Porro, A. Chaves-Sanjuan, M. Nardini, O. Rauh, G. Thiel, A. Moroni, Fusicoccin Activates KAT1 channels by stabilizing their interaction with 14-3-3 proteins, Plant Cell 29 (2017) 2570–2580, https://doi.org/tpc.17.00375 [pii] 10.1105/tpc.17.00375 [doi].
B. Zhang, R. Karnik, S. Waghmare, N. Donald, M.R. Blatt, VAMP721 conformations unmask an extended Motif for K+ channel binding and gating control, Plant Physiol. 173 (2017) 536–551, https://doi.org/10.1104/pp.16.01549.
A. Honsbein, S. Sokolovski, C. Grefen, P. Campanoni, R. Pratelli, M. Paneque, Z. Chen, I. Johansson, M.R. Blatt, A tripartite SNARE-K+ channel complex mediates in channel-dependent K+ nutrition in Arabidopsis, Plant Cell 21 (2009) 2859–2877, https://doi.org/10.1105/tpc.109.066118.
R. Hedrich, S. Neimanis, G. Savchenko, H.H. Felle, W.M. Kaiser, U. Heber, Changes in apoplastic ph and membrane potential in leaves in relation to stomatal responses to $CO_2$, malate, abscisic acid or interruption of water supply, Planta 213 (2001) 594–601, https://doi.org/10.1007/s004250100524.
S. Sokolovski, A. Hills, R.A. Gay, M.R. Blatt, Functional interaction of the SNARE protein NtSyp121 in Ca2+ channel gating, Ca2+ transients and ABA signalling of stomatal guard cells, Mol. Plant 1 (2008) 347–358, https://doi.org/10.1093/mp/ssm029.
C. Grefen, Z. Chen, A. Honsbein, N. Donald, A. Hills, M.R. Blatt, A novel motif essential for SNARE interaction with the K(+) channel KC1 and channel gating in Arabidopsis, Plant Cell 22 (2010) 3076–3092, https://doi.org/10.1105/tpc.110.077768.
C. Eisenach, Z.H. Chen, C. Grefen, M.R. Blatt, The trafficking protein SYP121 of Arabidopsis connects programmed stomatal closure and $K^+$ channel activity with vegetative growth, Plant J. 69 (2012) 241–251, https://doi.org/10.1111/j.1365-313X.2011.04786.x.
A. Locascio, N. Andrés-Colás, J.M. Mulet, L. Yenush, Saccharomyces cerevisiae as a tool to investigate plant potassium and sodium transporters, Int J. Mol. Sci. 20 (2019a) 2133, https://doi.org/10.3390/ijms20092133.
A. Locascio, M.C. Marqués, G. García-Martínez, C. Corratgé-Faillie, N. Andrés-Colás, L. Rubio, J.A. Fernández, A.A. Véry, J.M. Mulet, L. Yenush, BCl2-Associated Athanogene4 regulates the KAT1 potassium channel and controls stomatal movement, Plant Physiol. 181 (2019b) 1277–1294, https://doi.org/10.1104/PP.19.00224.
G.C. Pagnussat, H.J. Yu, Q.A. Ngo, S. Rajani, S. Mayalagu, C.S. Johnson, A. Capron, L. F. Xie, D. Ye, V. Sundaresan, V.S. Gabriela C Pagnussat 1, Hee-Ju Yu, Quy A. Ngo, Sarojam Rajani, Sevugan Mayalagu, Cameron S. Johnson, Arnaud Capron, Li-Fen Xie, De Ye, Genetic and molecular identification of genes required for female gametophyte development and function in Arabidopsis, Development 132 (2005) 603–614, https://doi.org/10.1242/dev.01595.
T. Maruta, M. Yonemitsu, Y. Yabuta, M. Tamoi, T. Ishikawa, S. Shigeoka, Arabidopsis phosphomannose isomerase 1, but not phosphomannose isomerase 2, is essential for ascorbic acid biosynthesis, J. Biol. Chem. 283 (2008) 28842–28851, https://doi.org/10.1074/jbc.M805538200.
A. Lebaudy, A. Vavasseur, E. Hosy, I. Dreyer, N. Leonhardt, J.B. Thibaud, A.A. Véry, T. Simonneau, H. Sentenac, Plant adaptation to fluctuating environment and biomass production are strongly dependent on guard cell potassium channels, Proc. Natl. Acad. Sci. USA 105 (2008) 5271–5276, https://doi.org/10.1073/pnas.0709732105.
A.E.I. Proudfoot, M.A. Payton, T.N.C. Wells, Purification and characterization of fungal and mammalian phosphomannose isomerases, J. Protein Chem. 13 (1994) 619–627, https://doi.org/10.1007/BF01890460.
F. Coulin, E. Magnenat, A.E.I. Proudfoot, M.A. Payton, P. Scully, T.N.C. Wells, Identification of Cys-150 in the active site of phosphomannose isomerase from Candida albicans, Biochemistry 32 (1993) 14139–14144, https://doi.org/10.1021/bi00214a010.
C.F. Kempinski, R. Haffar, C. Barth, Toward the mechanism of NH4+ sensitivity mediated by Arabidopsis GDP-mannose pyrophosphorylase, Plant Cell Environ. 34 (2011) 847–858, https://doi.org/10.1111/j.1365-3040.2011.02290.x.
M. He, C.Q. He, N.Z. Ding, Abiotic stresses: general defenses of land plants and chances for engineering multistress tolerance, Front Plant Sci. 871 (2018) 1–18, https://doi.org/10.3389/fpls.2018.01771.
J. Tao, H. Wu, Z. Li, C. Huang, X. Xu, Molecular evolution of gdp-d-mannose epimerase (gme), a key gene in plant ascorbic acid biosynthesis, Front Plant Sci. 9 (2018) 1–10, https://doi.org/10.3389/fpls.2018.01293.
C. Abeijon, C.B. Hirschberg, Topography of glycosylation reactions in the endoplasmic reticulum, Trends Biochem Sci. 17 (1992) 32–36, https://doi.org/10.1016/0968-0004(92)90424-8.
G.J. Seifert, Nucleotide sugar interconversions and cell wall biosynthesis: how to bring the inside to the outside, Curr. Opin. Plant Biol. 7 (2004) 277–284, https://doi.org/10.1016/j.pbi.2004.03.004.
C.J. Jeffery, Moonlighting proteins, Trends Biochem Sci. 24 (1999) 8–11, https://doi.org/10.1016/S0968-0004(98)01335-8.
G. Sriram, J.A. Martinez, E.R.B. McCabe, J.C. Liao, K.M. Dipple, Single-gene disorders: what role could moonlighting enzymes play? Am. J. Hum. Genet 76 (2005) 911, https://doi.org/10.1086/430799.
A.R. Robbins, R.D. Ward, C. Oliver, A mutation in glyceraldehyde 3-phosphate dehydrogenase alters endocytosis in CHO cells, J. Cell Biol. 130 (1995) 1093–1104, https://doi.org/10.1083/JCB.130.5.1093.
E.J. Tisdale, Glyceraldehyde-3-phosphate dehydrogenase is required for vesicular transport in the early secretory pathway, J. Biol. Chem. 276 (2001) 2480–2486, https://doi.org/10.1074/JBC.M007567200.
B. Su, Z. Qian, T. Li, Y. Zhou, A. Wong, PlantMP: a database for moonlighting plant proteins, 2019 (2019). https://doi.org/10.1093/DATABASE/BAZ050.
B. Moore, L. Zhou, F. Rolland, Q. Hall, W.H. Cheng, Y.X. Liu, I. Hwang, T. Jones, J. Sheen, Role of the Arabidopsis glucose sensor HXK1 in nutrient, light, and hormonal signaling, Science 300 (1979) (2003) 332–336, https://doi.org/10.1126/SCIENCE.1080585.
C. Rodríguez-Saavedra, L.E. Morgado-Martínez, A. Burgos-Palacios, B. King-Díaz, M. López-Coria, S. Sánchez-Nieto, Moonlighting proteins: the case of the hexokinases, Front Mol. Biosci. 8 (2021), https://doi.org/10.3389/FMOLB.2021.701975.
I. Turek, H. Irving, Moonlighting proteins shine new light on molecular signaling niches, Int J. Mol. Sci. 22 (2021) 1–22, https://doi.org/10.3390/IJMS22031367.
C.M. Paumi, J. Menendez, A. Arnoldo, K. Engels, K.R. Iyer, S. Thaminy, O. Georgiev, Y. Barral, S. Michaelis, I. Stagljar, Mapping protein-protein interactions for the yeast ABC transporter Ycf1p by integrated split-ubiquitin membrane yeast two-hybrid analysis, Mol. Cell 26 (2007) 15–25, https://doi.org/10.1016/j.molcel.2007.03.011.
P. Obrdlik, M. El-Bakkoury, T. Hamacher, C. Cappellaro, C. Vilarino, C. Fleischer, H. Ellerbrok, R. Kamuzinzi, V. Ledent, D. Blaudez, D. Sanders, J.L. Revuelta, E. Boles, B. Andre, W.B. Frommer, K+ channel interactions detected by a genetic system optimized for systematic studies of membrane protein interactions, 12242–7, Proc. Natl. Acad. Sci. 101 (2004), https://doi.org/10.1073/pnas.0404467101.
M.E. Lee, W.C. DeLoache, B. Cervantes, J.E. Dueber, A highly characterized yeast toolkit for modular, multipart assembly, ACS Synth. Biol. 4 (2015) 975–986, https://doi.org/10.1021/sb500366v.
A. Bertl, J. Ramos, J. Ludwig, H. Lichtenberg-Fraté, J. Reid, H. Bihler, F. Calero, P. Martínez, P.O. Ljungdahl, Characterization of potassium transport in wild-type and isogenic yeast strains carrying all combinations of trk1, trk2 tok1 Null. Mutat. 47 (2003) 767–780.
C. Navarrete, S. Petrezselyova, L. Barreto, J.L. Martinez, J. Zahradka, J. Arino, H. Sychrova, J. Ramos, Lack of main K plus uptake systems in Saccharomyces cerevisiae cells affects yeast performance in both potassium-sufficient and potassium-limiting conditions, FEMS Yeast Res 10 (2010) 508–517, https://doi.org/10.1111/j.1567-1364.2010.00630.x.
P.J. Cullen, J. Schultz, J. Horecka, B.J. Stevenson, Y. Jigami, G.F. Sprague, Defects in protein glycosylation cause SHO1-dependent activation of a STE12 signaling pathway in yeast, Genetics 155 (2000) 1005–1018.
J. Ramos, R. Haro, A. Rodriguez-Navarro, Regulation of potassium fluxes in Saccharomyces cerevisiae, Biochim. Et. Biophys. Acta (BBA) - Biomembr. 1029 (1990) 211–217, https://doi.org/10.1016/0005-2736(90)90156-I.
R.W. Gracy, E.A. Noltmann, Studies on phosphomannose isomerase. I. Isolation, homogeneity measurements, and determination of some physical properties. J. Biol. Chem. 243 (1968).
S.J. Clough, A.F. Bent, Floral dip: a simplified method for Agrobacterium-mediated transformation of Arabidopsis thaliana, Plant J. 16 (1998) 735–743.
F. Campos, J.R. Perez-Castiñeira, J.M. Villalba, F.A. Culiañez-Marciá, F. Sánchez, R. Serrano, Localization of plasma membrane H+-ATPase in nodules of Phaseolus vulgaris L, Plant Mol. Biol. 32 (1996) 1043–1053, https://doi.org/10.1007/BF00041388.
A. Sarrion-Perdigones, M. Vazquez-Vilar, J. Palací, B. Castelijns, J. Forment, P. Ziarsolo, J. Blanca, A. Granell, D. Orzaez, GoldenBraid 2.0: a comprehensive DNA assembly framework for plant synthetic biology, Plant Physiol. 162 (2013) 1618–1631, https://doi.org/10.1104/pp.113.217661.
J. Schindelin, I. Arganda-Carreras, E. Frise, V. Kaynig, M. Longair, T. Pietzsch, S. Preibisch, C. Rueden, S. Saalfeld, B. Schmid, J.Y. Tinevez, D.J. White, V. Hartenstein, K. Eliceiri, P. Tomancak, A. Cardona, Fiji: an open-source platform for biological-image analysis, Nat. Methods 9 (2012) 676–682, https://doi.org/10.1038/NMETH.2019.
K.J. Livak, T.D. Schmittgen, Analysis of relative gene expression data using real-time quantitative PCR and the 2(-Delta Delta C(T)) Method, Methods 25 (2001) 402–408, https://doi.org/10.1006/METH.2001.1262.
D.B. Duncan, Multiple range and multiple F tests, Biometrics 11 (1) (1955), https://doi.org/10.2307/3001478.
M.K. Swan, T. Hansen, P. Schönheit, C. Davies, Structural basis for phosphomannose isomerase activity in phosphoglucose isomerase from pyrobaculum aerophilum: a subtle difference between distantly related Enzymes †, Biochemistry 43 (2004) 40, https://doi.org/10.1021/bi048608y.
A. Bateman, M.J. Martin, S. Orchard, M. Magrane, R. Agivetova, S. Ahmad, E. Alpi, E. H. Bowler-Barnett, R. Britto, B. Bursteinas, H. Bye-A-Jee, R. Coetzee, A. Cukura, A. da Silva, P. Denny, T. Dogan, T.G. Ebenezer, J. Fan, L.G. Castro, P. Garmiri, G. Georghiou, L. Gonzales, E. Hatton-Ellis, A. Hussein, A. Ignatchenko, G. Insana, R. Ishtiaq, P. Jokinen, V. Joshi, D. Jyothi, A. Lock, R. Lopez, A. Luciani, J. Luo, Y. Lussi, A. MacDougall, F. Madeira, M. Mahmoudy, M. Menchi, A. Mishra, K. Moulang, A. Nightingale, C.S. Oliveira, S. Pundir, G. Qi, S. Raj, D. Rice, M. R. Lopez, R. Saidi, J. Sampson, T. Sawford, E. Speretta, E. Turner, N. Tyagi, P. Vasudev, V. Volynkin, K. Warner, X. Watkins, R. Zaru, H. Zellner, A. Bridge,

S. Poux, N. Redaschi, L. Aimo, G. Argoud-Puy, A. Auchincloss, K. Axelsen, P. Bansal, D. Baratin, M.C. Blatter, J. Bolleman, E. Boutet, L. Breuza, C. Casals-Casas, E. de Castro, K.C. Echioukh, E. Coudert, B. Cuche, M. Doche, D. Dornevil, A. Estreicher, M. L. Famiglietti, M. Feuermann, E. Gasteiger, S. Gehant, V. Gerritsen, A. Gos, N. Gruaz-Gumowski, U. Hinz, C. Hulo, N. Hyka-Nouspikel, F. Jungo, G. Keller, A. Kerhornou, V. Lara, P. Le Mercier, D. Lieberherr, T. Lombardot, X. Martin, P. Masson, A. Morgat, T.B. Neto, S. Paesano, I. Pedruzzi, S. Pilbout, L. Pourcel, M. Pozzato, M. Pruess, C. Rivoire, C. Sigrist, K. Sonesson, A. Stutz, S. Sundaram, M. Tognolli, L. Verbregue, C.H. Wu, C.N. Arighi, L. Arminski, C. Chen, Y. Chen, J.S. Garavelli, H. Huang, K. Laiho, P. McGarvey, D.A. Natale, K. Ross, C.R. Vinayaka, Q. Wang, Y. Wang, L. S. Yeh, J. Zhang, P. Ruch, D. Teodoro, UniProt: the universal protein knowledgebase in 2021, Nucleic Acids Res 49 (2021) D480–D489, https://doi.org/10.1093/NAR/GKAA1100.

M. Mirdita, K. Schütze, Y. Moriwaki, L. Heo, S. Ovchinnikov, M. Steinegger, ColabFold: making protein folding accessible to all, Nat. Methods 2022 19:6 19 (2022) 679–682, https://doi.org/10.1038/s41592-022-01488-1.

E.F. Pettersen, T.D. Goddard, C.C. Huang, G.S. Couch, D.M. Greenblatt, E.C. Meng, T. E. Ferrin, UCSF Chimera–a visualization system for exploratory research and analysis, J. Comput. Chem. 25 (2004) 1605–1612, https://doi.org/10.1002/JCC.20084.

S. Lu, J. Wang, F. Chitsaz, M.K. Derbyshire, R.C. Geer, N.R. Gonzales, M. Gwadz, D. I. Hurwitz, G.H. Marchler, J.S. Song, N. Thanki, R.A. Yamashita, M. Yang, D. Zhang, C. Zheng, C.J. Lanczycki, A. Marchler-Bauer, CDD/SPARCLE: the conserved domain database in 2020, Nucleic Acids Res 48 (2020) D265–D268, https://doi.org/10.1093/NAR/GKZ991.

A. Cleasby, A. Wonacott, T. Skarzynski, R.E. Hubbard, G.J. Davies, A.E.I. Proudfoot, A. R. Bernard, M.A. Payton, T.N.C. Wells, The X-ray crystal structure of phosphomannose isomerase from Candida albicans at 1.7 Å resolution, Nat. Struct. Biol. 1996 3:5 3 (1996) 470–479, https://doi.org/10.1038/nsb0596-470.

A. Rovira, N. Veciana, A. Locascio, L. Yenush, P. Leivar, E. Monte, PIF transcriptional regulators are required for rhythmic stomatal movements, (n.d.). https://doi.org/10.1101/2023.01.14.524044.

R. Niehues, M. Hasilik, G. Alton, C. Körner, M. Schiebe-Sukumar, H.G. Koch, K. P. Zimmer, R. Wu, E. Harms, K. Reiter, K. von Figura, H.H. Freeze, H.K. Harms, T. Marquardt, Carbohydrate-deficient glycoprotein syndrome type Ib. Phosphomannose isomerase deficiency and mannose therapy, J. Clin. Investig. 101 (1998) 1414–1420, https://doi.org/10.1172/JCI2350.

J. Jaeken, G. Matthijs, J.M. Saudubray, C. Dionisi-Vici, E. Bertini, P. De Lonlay, H. Henri, H. Carchon, E. Schollen, E. Van Schaftingen, Phosphomannose isomerase deficiency: a carbohydrate-deficient glycoprotein syndrome with hepatic-intestinal presentation, Am. J. Hum. Genet 62 (1998) 1535–1539, https://doi.org/10.1086/301873.

C. DeRossi, L. Bode, E.A. Eklund, F. Zhang, J.A. Davis, V. Westphal, L. Wang, A. D. Borowsky, H.H. Freeze, Ablation of mouse phosphomannose isomerase (Mpi) causes mannose 6-phosphate accumulation, toxicity, and embryonic lethality, J. Biol. Chem. 281 (2006) 5916–5927, https://doi.org/10.1074/JBC.M511982200.

F.A. Hoeberichts, E. Vaeck, G. Kiddle, E. Coppens, B. van de Cotte, A. Adamantidis, S. Ormenese, C.H. Foyer, M. Zabeau, D. Inzé, C. Périlleux, F. Van Breusegem, M. Vuylsteke, C. Pé rilleux, F. Van Breusegem, M. Vuylsteke, A Temperature-sensitive mutation in the Arabidopsis thaliana phosphomannomutase gene disrupts protein glycosylation and triggers cell death, J. Biol. Chem. 283 (2008) 5708–5718, https://doi.org/10.1074/JBC.M704991200.

P.L. Conklin, S.R. Norris, G.L. Wheeler, E.H. Williams, N. Smirnoff, R.L. Last, Genetic evidence for the role of GDP-mannose in plant ascorbic acid (vitamin C) biosynthesis, Proc. Natl. Acad. Sci. USA 96 (1999) 4198–4203, https://doi.org/10.1073/PNAS.96.7.4198/ASSET/7B648BE4-7CB3-4B68-A5A1-03F06C44E44B/ASSETS/GRAPHIC/PQ0690250006.JPEG.

G.L. Wheeler, M.A. Jones, N. Smirnoff, The biosynthetic pathway of vitamin C in higher plants, Nature 393 (1998) 365–369, https://doi.org/10.1038/30728.

M.W. Davey, M. Van Montagu, D. Inzé, M. Sanmartin, A. Kanellis, N. Smirnoff, I. J. Benzie, J.J. Strain, D. Favell, J. Fletcher, Review Plant L-ascorbic acid: chemistry, function, metabolism, bioavailability and effects of processing, J. Sci. Food Agric. 80 (2000) 825–860, https://doi.org/10.1002/(SICI)1097-0010(20000515)80:7%3C825::AID-JSFA598%3E3.0.CO;2-6.

P. Lerouge, M. Cabanes-Macheteau, C. Rayon, A.-C. Fischette-Lainé, V. Gomord, L. Faye, N-Glycoprotein biosynthesis in plants: recent developments and future trends, Plant Mol. Biol. 38 (1998) 31–48, https://doi.org/10.1023/A:1006012005654.

R.G. Spiro, Protein glycosylation: nature, distribution, enzymatic formation, and disease implications of glycopeptide bonds, Glycobiology 12 (2002), https://doi.org/10.1093/GLYCOB/12.4.43R.

A. Honsbein, M.R. Blatt, C. Grefen, A molecular framework for coupling cellular volume and osmotic solute transport control, J. Exp. Bot. 62 (2011) 2363–2370, https://doi.org/10.1093/jxb/erq386.

B. Zhang, R. Karnik, Y. Wang, N. Wallmeroth, M.R. Blatt, C. Grefen, The Arabidopsis R-SNARE VAMP721 interacts with KAT1 and KC1 K+ channels to moderate K+ current at the plasma membrane, Plant Cell 27 (2015) 1697–1717, https://doi.org/10.1105/tpc.15.00305.

C. Lefoulon, S. Waghmare, R. Karnik, M.R. Blatt, Gating control and K, Plant Cell Environ. 41 (2018) 2668–2677, https://doi.org/10.1111/pce.13392.

X. Chen, N.G. Irani, J. Friml, Clathrin-mediated endocytosis: the gateway into plant cells, Curr. Opin. Plant Biol. 14 (2011) 674–682, https://doi.org/10.1016/j.pbi.2011.08.006.

E.R. Larson, E. Van Zelm, C. Roux, A. Marion-Poll, M.R. Blatt, Clathrin Heavy Chain subunits coordinate endo- and exocytic traffic and affect stomatal movement, 00970.2017, Plant Physiol. 175 (2017), https://doi.org/10.1104/pp.17.00970.

J.U. Sutter, C. Sieben, A. Hartel, C. Eisenach, G. Thiel, M.R. Blatt, Abscisic acid triggers the endocytosis of the arabidopsis KAT1 K+ channel and its recycling to the plasma membrane, Curr. Biol. 17 (2007) 1396–1402, https://doi.org/10.1016/j.cub.2007.07.020.